


Article

An Insight into Flotation Chemistry of Pyrite with Isomeric Xanthates: A Combined Experimental and Computational Study

Guihong Han [†], Shengpeng Su [†], Yanfang Huang ^{*}, Weijun Peng ^{* }, Yijun Cao and Jiongtian Liu

School of Chemical Engineering and Energy, Zhengzhou University, Zhengzhou 450001, China; guihong-han@hotmail.com (G.H.); sspzsu@126.com (S.S.); yijuncao@126.com (Y.C.); scetljt@126.com (J.L.)

^{*} Correspondence: hlele114@163.com (Y.H.); pwj@zzu.edu.cn (W.P.)[†] These authors as co-first author contributed equally to this work.

Received: 26 March 2018; Accepted: 16 April 2018; Published: 19 April 2018



Abstract: The flotation chemistry between pyrite and isomeric xanthates (butyl xanthate and isobutyl xanthate) was investigated by means of adsorption experiments, surface tension tests, and molecular dynamic simulations in this work. The flotation chemical results were confirmed and further interpreted by quantum chemical calculations. The experiment results demonstrated that the isobutyl xanthate exhibited superior adsorption capacity and surface activity than those of butyl xanthate in flotation chemistry. In addition, molecular dynamic simulations were simultaneously performed in constant number, constant volume and temperature (NVT), and constant number, constant volume, and pressure (NPT) ensemble, indicating that the NPT ensemble was more suitable to the flotation system and the isobutyl xanthate was easier to be adsorbed on pyrite surface compared with butyl xanthate during an appropriate range of concentrations. Furthermore, the quantum chemical calculations elucidated that the isobutyl xanthate presented higher reactivity than that of the corresponding butyl xanthate based on the frontier molecular orbital theory of chemical reactivity, which was consistent with experimental and simulation results obtained. This work can provide theoretical guidance for an in-depth study of the flotation chemistry of pyrite with isomeric xanthates.

Keywords: pyrite; xanthates; flotation chemistry; molecular dynamic simulations; quantum chemical calculations

1. Introduction

High sulfur-containing bauxite is abundant in China. The amount of high sulfur-containing bauxite has reached 1.5×10^8 t [1]. The sulfur in high sulfur-containing bauxite, which is main in the form of pyrite [2], directly affects the process of alumina manufacture by the Bayer method [3]. Therefore, developing an economical and practical method for the removal of the sulfur is of great importance to industrial production. Desulfurization methods for high sulfur-containing bauxite have been intensively investigated over several decades, the proposed methods including flotation, roasting, and wet desulfurization, etc. [4–6]. In these methods, flotation desulfurization has been shown to be an effective method for the separation of sulfide minerals, which is widely used for the removal of pyrite [4]. Froth flotation is an important mineral processing method that utilizes the difference in wettability of mineral particles to concentrate valuable minerals [7]. Pyrite is readily floatable with several types of collectors: xanthates, dithiophosphates, fatty acids, etc. [8]. The xanthates series are the most importantly and widely used collectors in pyrite flotation [9]. Thus, it is necessary to understand the flotation chemistry of pyrite with xanthates during the flotation process.

Adsorption of xanthates on pyrite surface has attracted the attention of many investigators in the last 50 years [9–11]. Additionally, the adsorption mechanisms of xanthates onto pyrite

surface have been widely investigated by means of Fourier transform infrared spectroscopy (FTIR), X-ray photoelectron spectroscopy (XPS), secondary ion mass spectroscopy (SIMS), and electrochemical measurements [10,11]. At present, a general comprehension is that metal-xanthates, dixanthogen, and xanthate ions are co-adsorbed on pyrite surface [9]. Compared with the adsorption mechanisms, there are few studies on the effect of alkyl structure on the flotation chemistry of xanthate collectors. Cao et al. [12] investigated that the effect of alkyl structure on the flotation performance of xanthate collectors by means of density functional theory (DFT). It was found that the more the branched chains of carbon atoms attached to polar groups in isomer xanthates, the stronger the flotation activity was, which was also further confirmed by another group [13,14] via froth flotation and biodegradability of alkyl xanthate collectors. The results of these studies demonstrated the branched chains have a significant effect on the flotation performance of xanthates. Furthermore, isobutyl xanthate exhibits a greater activity and stability than those of the corresponding butyl xanthate. However, to the best of our knowledge, little attention has been paid to the flotation chemistry of pyrite with butyl xanthate and isobutyl xanthate at a molecule level.

In recent years, molecular dynamic (MD) simulations is a valuable tool to study the adsorption of surfactants on solid surfaces at the microscopic level [15–17], which makes it possible to accurately interpret the flotation chemistry of the collector on solid–water interface through constructing a computational model that tends to real flotation environment. Moreover, MD simulations can elucidate the dynamic characteristics of the flotation process [18]. Wang et al. [19] revealed that the dodecylamine molecules adsorbed on muscovite surface by electrostatic interactions and hydrogen bonding, while the oleate molecules could co-adsorb with the dodecylamine molecules on the muscovite surface by MD simulations.

The objective of the present investigation is to understand the underlying flotation chemistry of pyrite with butyl xanthate and isobutyl xanthate by experiments and MD simulations at the microscopic level. The aqueous solution and complex flotation systems containing different xanthate concentrations were constructed by Materials Studio 8.0, and the MD simulations between pyrite and isomeric xanthates were implemented using the Forcite module. Furthermore, the flotation chemical results were further elucidated by focusing on the quantum chemical calculations based on density function theory (DFT). This study can be helpful to understand the flotation chemistry of pyrite with butyl xanthate and isobutyl xanthate.

2. Materials and Methods

2.1. Materials

A pure mineral sample of pyrite was obtained from Tongling Mine, Anhui Province, China. Then the pyrite was sieved to give different particle size fractions using a standard sieve, and a part of the pyrite with the particle size fraction of 45–75 μm was sampled in the experiments. The sample was kept in a dryer to prevent further surface oxidation and ensure reproducibility of the tests. The crystal phase of FeS_2 was verified by X-ray diffraction (XRD). As shown in Figure 1, no impurity peaks were observed, confirming the high purity of the FeS_2 crystal.

Butyl xanthate and isobutyl xanthate were synthesized by reacting butyl alcohol or isobutyl alcohol with sodium hydroxide and carbon disulfide in the laboratory, which were purified by three cycles of dissolution in acetone and recrystallization with petroleum ether [20]. All the other reagents used in this study were analytical grade and used without further purification. Deionized water was used for all experiments.

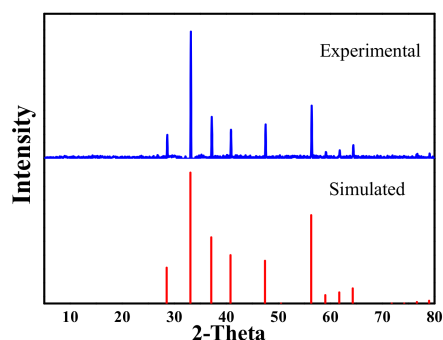


Figure 1. X-ray diffraction (XRD) pattern of the pyrite sample.

2.2. Experimental

2.2.1. Adsorption Procedure

Kinetic studies were implemented by mixing an accurate mass of 50 ± 0.01 mg pyrite to a series of 100 ± 1 mL conical flasks filled with 25 ± 0.01 mL of 1 mmol/L diluted solutions. For sorption isotherms experiments, suspensions contained 500 ± 0.01 mg pyrite in 25 ± 0.01 mL xanthate solutions in the range of 0–40 mmol/L. Full details of the adsorption procedure were given in the Supporting Information file. The amount of xanthates adsorbed on pyrite surface at equilibrium q_e (mmol/g) was calculated according to the following equation:

$$q_e = \frac{(C_0 - C_e)V}{m} \quad (1)$$

where C_0 , C_e (mmol/L) corresponds to the initial and equilibrium concentrations of xanthates in solution, respectively. V is the volume (L) of the solution, and m is the mass of adsorbent used (g).

2.2.2. Surface Tension Testing

Surface tension measurements were conducted by the pendant drop (PD) method using a JC2000D1 contact angle measuring instrument (POWEREACH, Shanghai, China). A small amount of liquid was required, and a controlled atmosphere inside the measuring cell was easily achieved [21]. The temperature was maintained at 25 °C by circulating thermostated water through a jacketed vessel that contained the solution during the measurements. Each sample was allowed to attain equilibrium for 10 min at each measurement [22]. The measurements were taken until surface tension values were constant, which demonstrated that the equilibrium had been reached [23]. In order to ensure the accuracy of the parameters, all experiments were repeated at least three times to obtain the average. The values of the surface tension at the CMC (γ_{cmc}) and the critical micelle concentration (CMC) were determined from the intersection of the two straight lines drawn in low and high concentration regions in surface tension curves (γ - C curves) via a linear regression analysis method [24].

2.3. Theory Calculations

All simulations were implemented using the Forcite module in the commercial Materials Studio software package (Accelrys Software Inc. (2016) Materials studio modeling environment, Release 8.0. Accelrys Software Inc., San Diego, CA, USA). MD simulations were carried out in a simulation box with periodic boundary conditions (PBC) via the universal force field [25], which is a full periodic table force field for molecular mechanics and MD simulations. A detailed explanation of the universal force field was given in the Supporting Information file.

Cheng et al. [26] reported that the water molecules adsorbed on pyrite surface resulted in the change of structure and electronic properties of sulfide minerals by DFT. Thus, MD simulations were performed to investigate the interaction between pyrite surface and isomeric xanthates in aqueous

solution. Moreover, considering the importance of other flotation reagents in the flotation system, a simulation box with the dimensions of $22.03 \times 22.03 \times 46.05 \text{ \AA}^3$, containing copper sulfate as an activator and terpineol as a frother, was constructed. The MD simulations were carried out in NVT or NPT ensemble using the Hoover-Nosé algorithm at 298 K because the ensemble could not be ascertained on the basis of existing literatures [17,19,27,28]. The minimization was performed using the Smart algorithm that automatically combines appropriate features of the other available methods in a cascade [29]. The Ewald summation method [30] and a cut off of 1.25 nm were used to calculate the non-bonded interactions (Vander Waals and Coulomb interactions). Finally, 10 ns simulations were conducted to relax the system fully, and the trajectories of the last 1 ns were used for analysis [17]. Full details of simulation methods were given in the Supporting Information file.

The potential energies were obtained by computing the energy of equilibration configurations. The relative affinity of the interactions between mineral surface and xanthates solution were quantified in terms of interaction energy, calculated using the following expression [31]:

$$\Delta E = E_{total} - E_{surface} - E_{xanthate} \quad (2)$$

where E_{total} is the total energy of the pyrite crystal together with the adsorbed xanthate molecules in solution and $E_{surface}$, $E_{xanthate}$ is the total energy of the pyrite surface and xanthate solution, respectively. It is worth noting that increasingly negative interaction energy (ΔE) values indicate more favorable interactions between the pyrite surface and the xanthate solutions [32].

Besides, quantum chemical calculations for the pyrite and isomeric xanthates were performed using the DMol3 module. The structures of the pyrite and xanthates were geometrically optimized by DFT with DNP basis set [33]. Details of the DFT calculations were given in the Supporting Information file.

3. Results and Discussion

3.1. Flotation Solution Chemistry between Pyrite and Isomeric Xanthates

3.1.1. Adsorption of Isomeric Xanthates onto Pyrite Surface

Adsorption kinetics and isotherms of xanthates on pyrite surface are presented in Figure 2. As shown in Figure 2a, it is observed that there is a dramatic increase during starting stage of adsorption, until the adsorption process reaches equilibrium after 10 min. Compared with butyl xanthate, the adsorption rate of isobutyl xanthate is higher under identical conditions. It is noticeable that the equilibrium adsorption amount q_e (mmol/g) of isobutyl xanthate is almost equal to that of butyl xanthate due to the lower concentration of xanthate solutions during adsorption process.

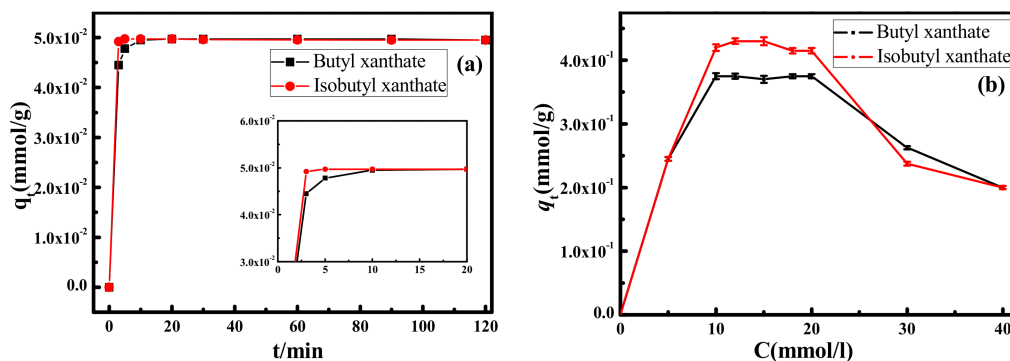


Figure 2. Adsorption kinetics (a) and isotherms (b) of xanthates on pyrite surface.

To evaluate the influences of xanthate concentration on the adsorption process, the adsorption of xanthates onto pyrite surface were implemented at various concentrations (from 0 to 40 mmol/L). As can be observed in Figure 2b, the equilibrium adsorption capacity q_e (mmol/g) of butyl xanthate and isobutyl xanthate are increasing gradually, which reach 0.375 ± 0.005 and 0.430 ± 0.005 mmol/g in the range of 10–20 mmol/L, respectively. However, outweighing 20 mmol/L, the equilibrium adsorption capacity q_e (mmol/g) declines gradually, which is attributed to the super saturation of the xanthate solution on pyrite surface, increasing the electrostatic repulsion force between molecules [34].

3.1.2. Surface Activity of Isomeric Xanthates in Flotation Chemistry

Generally speaking, a surfactant simultaneously consists of hydrophilic and hydrophobic groups [35]. The hydrophobic groups of surfactants play an essential role in adjusting surface activity for attaching to air bubbles. Besides, surfactants are powerful enough to reduce the surface tension of the solution, which could be beneficial to form stable bubbles for enhancing the attachment of air bubbles to the hydrophobized mineral particles, leading to an increase of recovery of the mineral particles [36].

In order to further explain the flotation performance of isomeric xanthates, it would be of interest and importance to investigate the surface activity of xanthates in flotation chemistry. Figure 3 shows the surface tension (γ) versus concentration (C) plot obtained from the xanthates solutions before and after adsorption at 298 K. It is clearly seen that the surface tensions gradually decrease with the increase of the xanthates concentration to a plateau region, above which a nearly constant value (γ_{cmc}) is obtained.

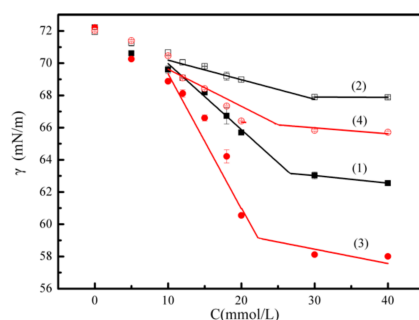


Figure 3. Surface tension as a function of the concentration of xanthates solution at 298 K (butyl xanthate ■; isobutyl xanthate ●; initial (1), (3); equilibrium (2), (4)).

The parameters values determined from the surface tension data are reported in Table 1. As shown in Table 1, the CMC values decrease on going from butyl xanthate to isobutyl xanthate due to the different chemical structure of hydrocarbon chains [12]. Besides, it is evident that the γ_{cmc} values of butyl xanthate are greater than that of isobutyl xanthate because of different chemical structures of the hydrocarbon chains. Thus, the isobutyl xanthate exhibits a greater surface activity compared with butyl xanthate in flotation chemistry.

Table 1. Activity parameters of xanthates at 298 K.

Xanthate		CMC (mmol/L)	γ_{cmc} (mN/m)	Π_{cmc} (mN/m)	Γ_{max} ($\mu\text{mol}/\text{m}^2$)	A_{min} (\AA^2)
After adsorption	Butyl xanthate	29.7 ± 0.2	67.9 ± 0.1	4.15 ± 0.1	48.9 ± 0.57	3.40 ± 0.29
	Isobutyl xanthate	25.3 ± 0.2	66.1 ± 0.1	5.95 ± 0.1	92.8 ± 2.6	1.79 ± 0.064
Before adsorption	Butyl xanthate	26.5 ± 0.2	63.1 ± 0.1	8.86 ± 0.1	165.2 ± 2.3	1.01 ± 0.072
	Isobutyl xanthate	22.2 ± 0.2	59.2 ± 0.1	10.9 ± 0.1	338.2 ± 6.6	0.491 ± 0.025

From the surface tension plots, the effectiveness of surface tension reduction, Π_{cmc} can be obtained. Π_{cmc} is the surface pressure at the CMC, being defined by

$$\Pi_{cmc} = \gamma_0 - \gamma_{cmc} \quad (3)$$

where γ_0 is the surface tension of pure solvent and γ_{cmc} is the surface tension of the solution at the CMC.

Parameter Π_{cmc} indicates the maximum reduction of surface tension caused by the dissolution of xanthate molecules, hence, becomes a measure for the effectiveness of the surfactant to lower the surface tension of the solvent [24]. The values of Π_{cmc} obtained for the xanthates are summarized in Table 1 together with the CMC and γ_{cmc} values. It can be seen that the Π_{cmc} increases in value following the sequence of butyl xanthate, isobutyl xanthate, which demonstrates that isobutyl xanthate is superior to butyl xanthate in the effectiveness of surface tension reduction (Π_{cmc}).

By applying the Gibbs adsorption isotherm to the surface tension versus concentration plot in the concentration range below the CMC, the maximum surface excess concentration, Γ_{max} , and the area occupied by a single surfactant molecule at the air-water interface, A_{min} , can be estimated [24]. The Gibbs equation for monovalent ionic surfactants is given by

$$\Gamma = -\frac{1}{RT} \left(\frac{d\gamma}{dC} \right)_T \quad (4)$$

where R is the gas constant (8.314 J/(mol·K)), T is the absolute temperature, and C is the xanthates concentration in bulk solution. When Γ_{max} is obtained, A_{min} value is estimated from the following relation:

$$A_{min} = \frac{1}{N_A \cdot \Gamma_{max}} (\times 10^{23} \text{ \AA}) \quad (5)$$

where N_A is the Avogadro constant (6.022×10^{23} mol/L).

When the xanthate molecules are adsorbed on the solution surface, isobutyl xanthate has a larger surface coverage than that of butyl xanthate attributed to the surface energy of the isomeric alkyl group is smaller than that of the n-alkyl group [37]. Therefore, the greater the Γ_{max} , the smaller the A_{min} , resulting in the more surfactant molecules adsorbed on the surface and the lower the surface tension obtained. It is isobutyl xanthate that has a greater surface activity compared with butyl xanthate in the flotation chemistry. These results demonstrate that isobutyl xanthate may be more beneficial to form stable bubbles for enhancing the attachment of air bubbles to the mineral particles, leading to an increase of recovery of the mineral particles.

3.2. MD Simulations between Pyrite and Isomeric Xanthates

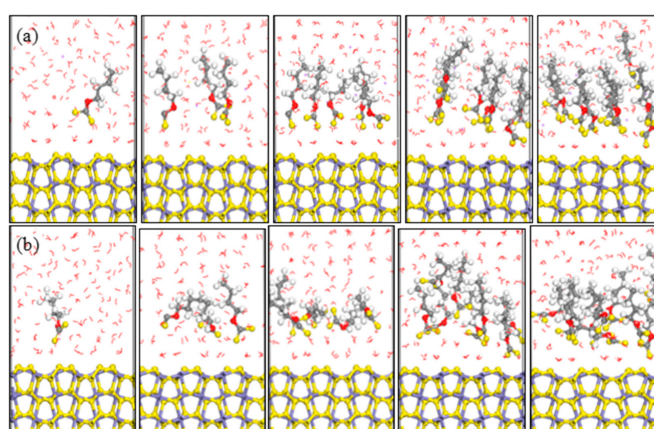
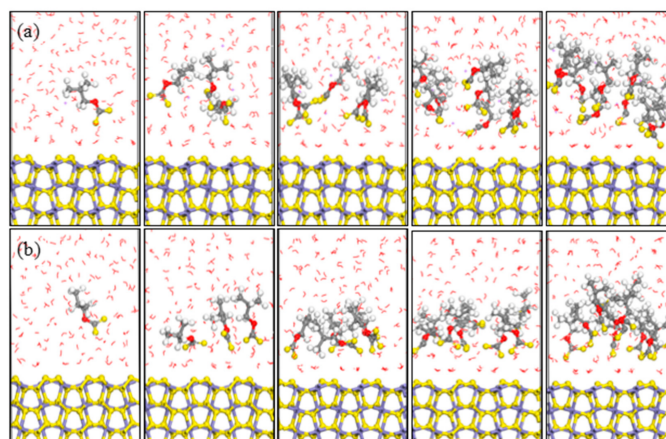
3.2.1. Interactions between Pyrite and Isomeric Xanthates without Frother and Activator

Based on the results of the flotation solution chemistry, pyrite particles are dispersed in water, and xanthate ions generated by ionization are the effective component that may be adsorbed on the pyrite surface [12]. Thus, MD simulations were performed first to compare the adsorption energies of H₂O, butyl xanthate, and isobutyl xanthate ions alone on the pyrite surface in the vacuum, and the results are summarized in Table 2. As is evidenced in Table 2, the adsorption energy of H₂O onto pyrite (100) plane is -26.45 ± 1.2 kJ/mol, wherefore the H₂O molecule can be adsorbed on pyrite (100) surface spontaneously, which is consistent with the contact angle results obtained by Monte et al. [38]. Furthermore, the adsorption energy of isobutyl xanthate is higher than that of butyl xanthate, and the value is -104.76 ± 2.5 and -100.79 ± 2.6 kJ/mol, respectively. By comparison, the adsorption energy of butyl xanthate and isobutyl xanthate are approximate triple more than that of H₂O. The more negative adsorption energy are, the stronger interactions between xanthates and pyrite surface is, which makes it easy for butyl xanthate and isobutyl xanthate ions to replace the adsorbed H₂O onto pyrite surface, leading to the hydrophobicity of the pyrite surface.

Table 2. Comparison of adsorption energies of different adsorbates on pyrite (100) surface (kJ/mol).

Adsorbate	Butyl Xanthate Ion	Isobutyl Xanthate Ion	H ₂ O
Adsorption energy	-100.79 ± 2.6	-104.76 ± 2.5	-26.45 ± 1.2

MD simulations of xanthates adsorbed on pyrite (100) surface were performed in an attempt to understand the interactions between pyrite surface and various xanthate concentrations in aqueous solutions. The optimized equilibrium configurations between pyrite surface and xanthates were shown in Figures 4 and 5. According to the equilibrium configuration of the different xanthates adsorbed on pyrite (100) surface, it was found that the hydrophilic head groups of xanthates were adsorbed on the pyrite surface, which demonstrated that xanthate anions were the effective component during the flotation process. The hydrophobic groups of xanthate stretch toward the solution and form a hydrophobic membrane, producing a hydrophobic state.

**Figure 4.** Equilibrium configurations of different butyl xanthate concentrations on pyrite surface in aqueous solution (a) NVT; (b) NPT; (Color codes: red = O, white = H, yellow = S, grey = C, iron grey = Fe, purple = Na; The above pictures is 1, 3, 5, 8, and 10 numbers of xanthate, respectively).**Figure 5.** Equilibrium configurations of different isobutyl xanthate concentrations on pyrite surface in aqueous solution (a) NVT; (b) NPT; (Color codes: red = O, white = H, yellow = S, grey = C, iron grey = Fe, purple = Na; The above pictures is 1, 3, 5, 8, and 10 numbers of xanthate, respectively).

All equilibration configurations obtained were used to compute the total potential energies of the MD systems and interaction energies between pyrite surface and xanthate solutions, which can be compared relatively within a given set of simulations but not to experimental values [39]. The potential

energy and interaction energy between pyrite surface and different xanthate concentrations were displayed in Figure 6. As can be seen from Figure 6a,b, the interactions between pyrite surface and xanthate solutions rise gradually and then decline due to the electrostatic repulsion of xanthates adsorbed on pyrite surface. As shown in Table 3, it is obvious that the electrostatic repulsion are rising dramatically due to the increase of xanthate concentrations, resulting in the decrease of the interaction energies. In addition, the interaction energy between pyrite surface and isobutyl xanthate is greater than that of butyl xanthate in Figure 6b. By comparison, the interaction energies of butyl xanthate and isobutyl xanthate with pyrite in Figure 6d are in compliance with the results in Figure 6b. Moreover, the interaction energies are larger for NPT ensemble. However, there is a large difference in total potential energies for NVT or NPT ensemble in Figure 6a,c. The interpretation could be deduced as follows. For NVT ensemble, the volume of the system being fixed, the pressure of the system rises gradually with the increase of xanthate concentrations, thus the total potential energies rise gradually and then decline because of the electrostatic repulsion. With the pressure of the system being fixed, the volume of the system can change for NPT ensemble. It can be found that the volume of the system has a slight rise with increase of xanthate concentrations. Compared with NVT ensemble, the system can relax completely in NPT ensemble, and the electrostatic repulsion is smaller. In conclusion, the system of NPT ensemble may be more stable for the interaction between xanthate and pyrite. Therefore, we will apply this method in subsequent research. These results demonstrate that the adsorption of isobutyl xanthate on the pyrite surface is easier, which is consistent with adsorption experimental results that we obtained.

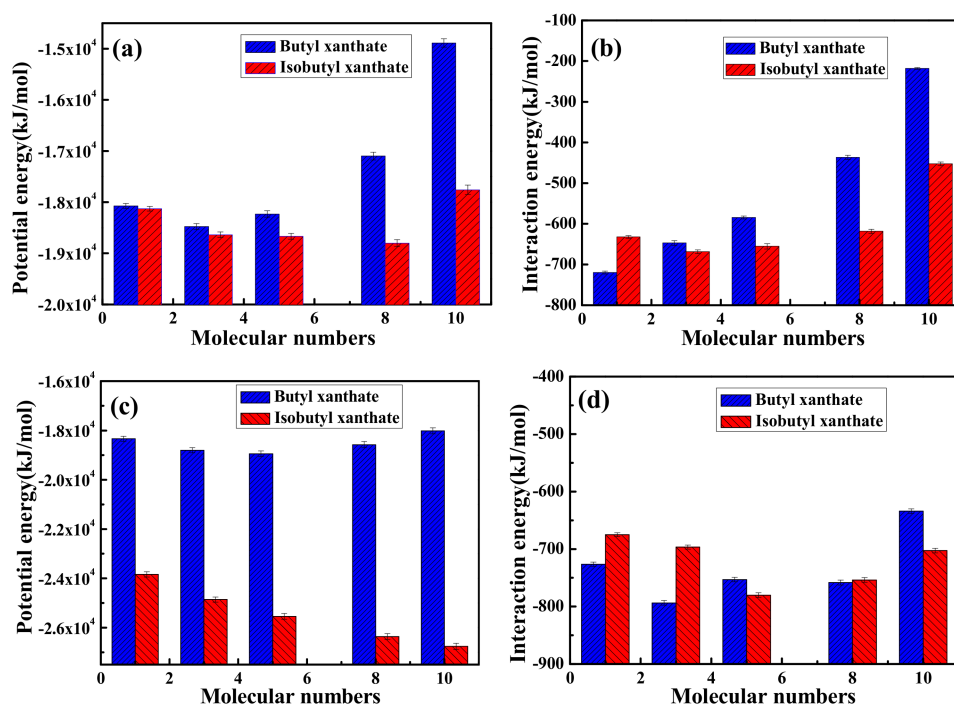


Figure 6. Potential and Interaction energies between pyrite surface and xanthate solution for NVT (a,b) ensemble or NPT; (c,d) ensemble.

Table 3. Electrostatic energies of different xanthate concentrations in aqueous solution for NVT or NPT ensemble (kJ/mol).

Ensemble	Numbers of Xanthates	1	3	5	8	10
NVT	Butyl xanthate	-2837.43 ± 92.93	-3605.57 ± 109.18	-4254.63 ± 118.41	-5065.44 ± 140.39	-5364.72 ± 151.69
	Isobutyl xanthate	-2736.72 ± 88.93	-3606.63 ± 104.61	-4238.93 ± 105.77	-5335.12 ± 117.29	-5720.40 ± 154.66
NPT	Butyl xanthate	-2694.52 ± 93.42	-3352.89 ± 97.58	-4051.46 ± 100.27	-4768.22 ± 105.37	-5224.37 ± 113.88
	Isobutyl xanthate	-2651.09 ± 92.01	-3328.48 ± 96.51	-4052.44 ± 99.89	-5126.57 ± 107.28	-5725.45 ± 111.37

3.2.2. Interactions between Pyrite and Isomeric Xanthates in the Presence of Frother and Activator

The optimized equilibrium configurations of butyl xanthate and isobutyl xanthate onto pyrite surface in the flotation chemistry are shown in Figures 7 and 8. The total potential energy and interaction energy between pyrite and different concentration xanthates are also reported in Figure 9. As can be observed in Figures 7 and 8, the adsorption behaviors of xanthates on pyrite surface are similar to the results in aqueous solution. However, the interaction energies are positive for 8 and 10 numbers of xanthate solutions in Figure 9b, attributed to the greater electrostatic repulsion compared with aqueous solution, which is verified by the results of the electrostatic energies in Table 4. For NPT ensemble, the interaction energies are larger than that of NVT ensemble. In addition, the potential energies rise with the increase of xanthate concentrations, because the volume of the system rises slightly with increase of xanthate concentrations. The system can relax completely for constant pressure, and the electrostatic repulsion is smaller. These results reveal that isobutyl xanthate presents greater flotation performance in aqueous solution and flotation chemistry.

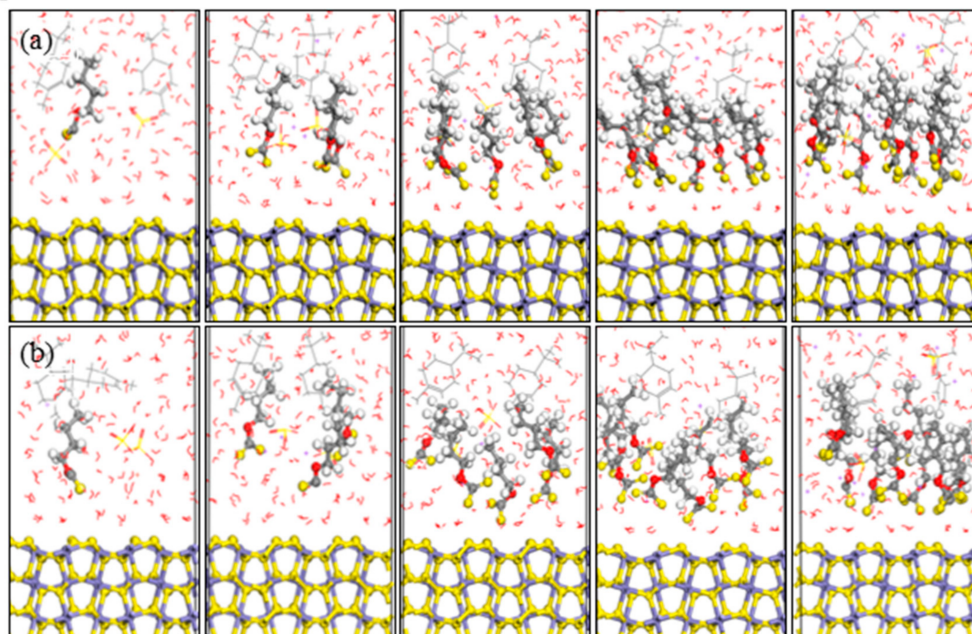


Figure 7. Equilibrium configurations of different butyl xanthate concentrations on pyrite surface in flotation chemistry (a) NVT; (b) NPT; (Color codes: red = O, white = H, yellow = S, grey = C, iron grey = Fe, purple = Na, brown = Cu; The above pictures is 1, 3, 5, 8, and 10 numbers of xanthate, respectively).

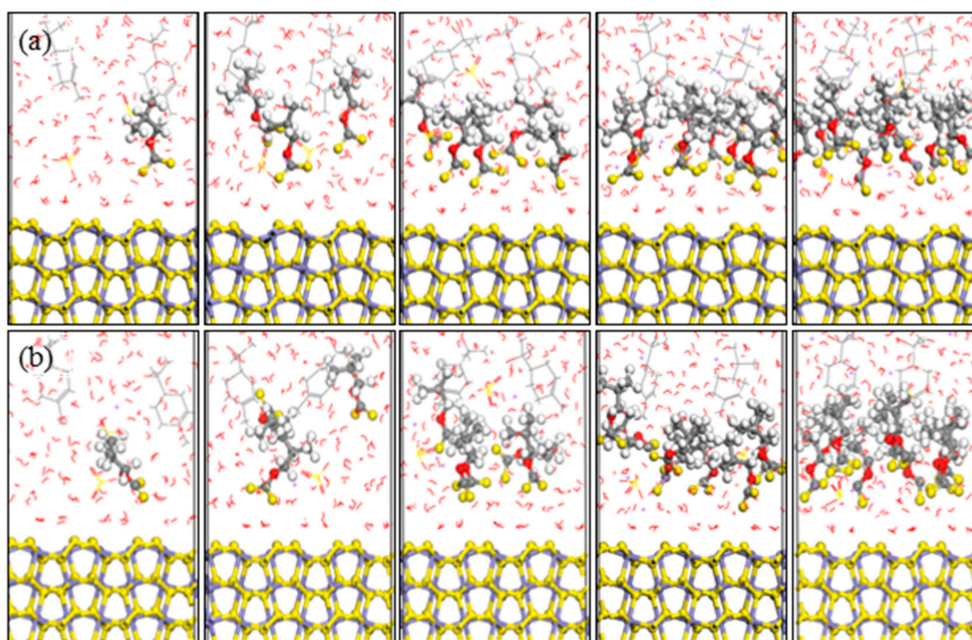


Figure 8. Equilibrium configurations of different isobutyl xanthate concentrations on pyrite surface in flotation chemistry (a) NVT; (b) NPT; (Color codes: red = O, white = H, yellow = S, grey = C, iron grey = Fe, purple = Na, brown = Cu; The above pictures is 1, 3, 5, 8, and 10 numbers of xanthate, respectively).

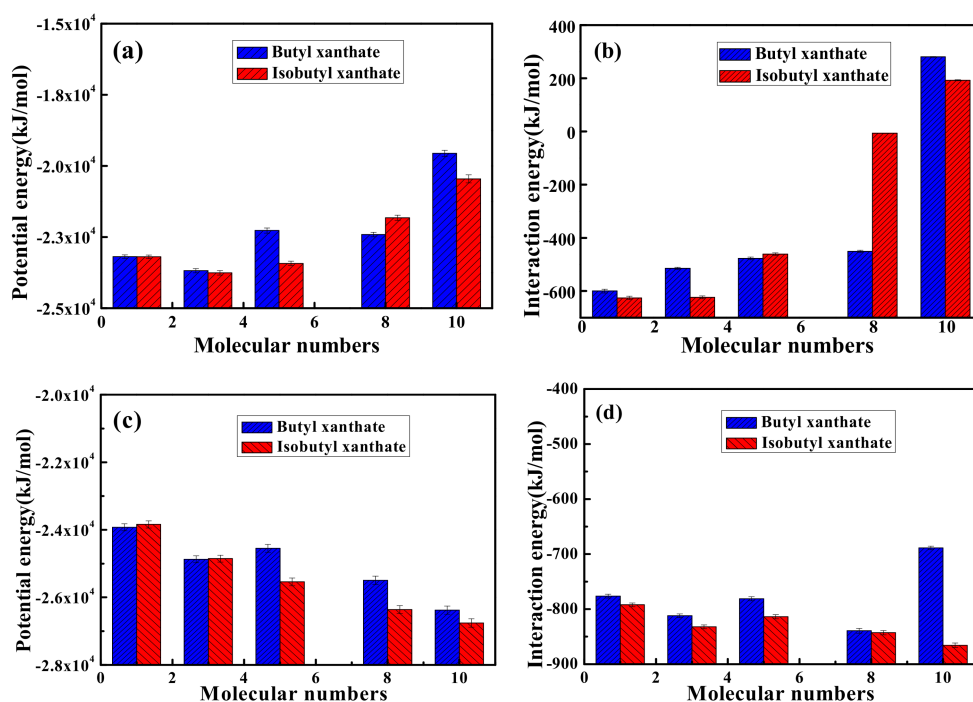


Figure 9. Potential and Interaction energies between pyrite surface and xanthate solution for NVT (a,b) ensemble or NPT (c,d) ensemble.

Table 4. Electrostatic energies of different xanthate concentrations in the flotation chemistry for NVT or NPT ensemble (kJ/mol).

Ensemble	Numbers of Xanthates	1	3	5	8	10
NVT	Butyl xanthate	$-10,393.07 \pm 115.01$	$-12,286.21 \pm 132.44$	$-12,730.93 \pm 168.57$	$-14,779.68 \pm 142.91$	$-18,323.18 \pm 162.99$
	Isobutyl xanthate	$-10,471.61 \pm 111.32$	$-12,241.89 \pm 135.85$	$-14,007.95 \pm 141.68$	$-16,591.48 \pm 147.31$	$-18,559.74 \pm 200.99$
NPT	Butyl xanthate	$-10,367.21 \pm 103.21$	$-12,051.86 \pm 103.70$	$-12,559.27 \pm 116.23$	$-14,436.87 \pm 125.32$	$-18,229.68 \pm 122.63$
	Isobutyl xanthate	$-10,211.36 \pm 104.24$	$-12,013.49 \pm 103.70$	$-13,941.43 \pm 113.77$	$-16,443.92 \pm 117.75$	$-18,347.99 \pm 125.90$

3.3. Quantum Chemical Calculations between Pyrite and Isomeric Xanthates

Quantum chemical calculation is an important method to study the correlation between adsorption mechanism and molecular structure in the flotation field [40]. Thus, DFT was carried out to explain the differences of flotation performances of butyl xanthate and isobutyl xanthate with pyrite in the present work. Additionally, according to the frontier molecular orbital theory (FMO) of chemical reactivity [41], transition of electron is due to interactions between highest occupied molecular orbital (HOMO) and lowest unoccupied molecular orbital (LUMO) of reacting species. In terms of pyrite, the reaction is the HOMO orbit of the xanthate and the LUMO orbit of the pyrite [42]. $\Delta E_1 = E_{\text{xanthate HOMO}} - E_{\text{pyrite LUMO}}$. The smaller the absolute value of ΔE_1 is, the greater effect of the reagent on the mineral has [12]. The density distribution of the frontier molecule orbital of butyl xanthate and isobutyl xanthate are shown in Figure 10. Moreover, the corresponding quantum chemical parameters including energy of the xanthate molecules orbital (E_{HOMO} , E_{LUMO}), energy gap ($\Delta E_2 = E_{\text{LUMO}} - E_{\text{HOMO}}$), and dipole moment (μ) from the optimized structures are summarized in Table 5.

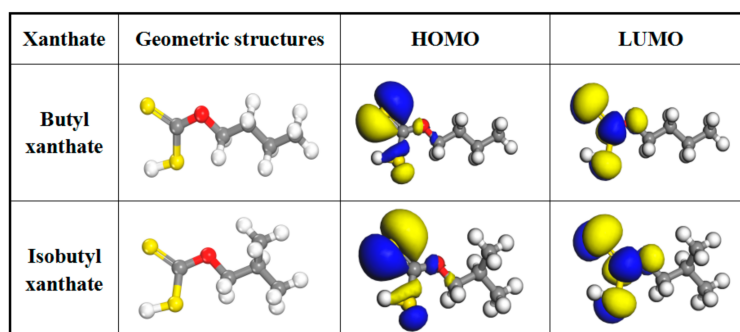


Figure 10. Optimized molecular structures and frontier molecular orbital of butyl xanthate and isobutyl xanthate (Color codes: red = O, yellow = S, white = H and gray = C).

As can be seen from Figure 10, the HOMO is mainly distributed in the double bond sulfur atom of xanthate molecules, while the LUMO is mostly located at the hydrophilic group, which demonstrates that xanthate anions are the active component during flotation process. Moreover, the energy gap ($\Delta E_2 = E_{\text{LUMO}} - E_{\text{HOMO}}$) reflects the chemical stability of xanthate molecules, and a lower value of ΔE shows that the investigated xanthates can be adsorbed easily on pyrite surface [43]. As shown in Table 5, the energy of the HOMO is -5.214 eV for butyl xanthate and -5.058 eV for isobutyl xanthate, respectively, and the values of energy gap ($\Delta E_2 = E_{\text{LUMO}} - E_{\text{HOMO}}$) are found to be 3.040 eV for butyl xanthate and 2.975 eV for isobutyl xanthate. In addition, the energy gap for isobutyl xanthate-pyrite system is smaller than that of butyl xanthate-pyrite, with the values being respectively 0.049 eV and 0.261 eV. These results show that isobutyl xanthate can be adsorbed easily on pyrite surface.

Table 5. Frontier orbital energy of xanthates and pyrite.

	The Energy of Molecule Orbital/eV		Energy Gap/eV		μ/Debye
	HOMO	LUMO	$ \Delta E_1 $	$ \Delta E_2 $	
Pyrite	-5.878	-4.438	-	-	-
Butyl xanthate	-5.214	-2.174	0.776	3.040	3.845
Isobutyl xanthate	-5.058	-2.083	0.620	2.975	4.012
Butyl xanthate-pyrite	-5.399	-5.318	-	0.261	-
Isobutyl xanthate-pyrite	-5.287	-5.238	-	0.049	-

Notes: $\Delta E_1 = |E_{\text{HOMO}}^{\text{xanthate}} - E_{\text{LUMO}}^{\text{pyrite}}|$; $\Delta E_2 = |E_{\text{HOMO}}^{\text{xanthate}} - E_{\text{LUMO}}^{\text{xanthate}}|$.

The greater value of μ leads to stronger adsorption due to electronic force [44]. The total dipole moment μ of molecular is a parameter characterizing the interactions between molecules. With the increasing of μ , it becomes easier for isobutyl xanthate to be adsorbed on the pyrite surface. Table 5 shows the values of μ of both the molecules are great, especially for isobutyl xanthate. These results confirm that isobutyl xanthate is easily adsorbed on the pyrite surface, which is agreement with aforementioned experiments and MD simulations results.

4. Conclusions

The experiments and theory calculations were adopted to study the flotation chemistry between pyrite and isomeric xanthates in this work. The adsorption experiment results demonstrated that more isobutyl xanthate could be adsorbed on pyrite surface. Compared with butyl xanthate, the isobutyl xanthate showed smaller CMC, γ_{cmc} , A_{min} and greater Π_{cmc} , Γ_{max} , which indicated that isobutyl xanthate exhibited greater surface activity than that of butyl xanthate. Additionally, the molecular dynamic simulations results illustrated that the system of NPT ensemble may be more appropriate for the interaction between xanthate and pyrite, and isobutyl xanthate presented superior flotation performance than that of butyl xanthate during an appropriate range of concentrations in aqueous solution and flotation chemistry. However, the flotation performances decreased dramatically due to the excess of xanthates adsorbed on pyrite surface, which was verified by adsorption experiments and electrostatic interactions. Furthermore, quantum chemical calculation also revealed that the isobutyl xanthate exhibited higher reactivity compared with butyl xanthate, which was in good agreement with experimental and simulation results obtained.

Acknowledgments: The authors acknowledge the financial support of the National Science Fund of China (No. 51674225, No. 51774252, No. 51404213, and No. 51404214), the National Sci-Tech Support Plan of China (2014BAB01B02), the China Postdoctoral Science Foundation (No. 2017M622375), the Educational Commission of Henan Province of China (No. 17A450001, No. 18HASTIT011, and No. 18A450001), the Development Fund for Outstanding Young Teachers of Zhengzhou University (No. 1421324065), and the Supercomputer Center in Zhengzhou University.

Author Contributions: Shengpeng Su conceived and designed the experiments, performed the calculation and wrote this paper under the supervision of Guihong Han and Yanfang Huang. Weijun Peng revised the manuscripts. Jiongtian Liu and Yijun Cao contributed analysis tools.

Conflicts of Interest: The authors declare no conflict of interest.

References

1. He, B.Q.; Luo, L. Discussion on the new de-sulfuration method of Chinese high sulfur bauxite. *Light Metal* **1996**, *12*, 3–5.
2. Hu, X.L.; Chen, W.M.; Xie, Q.L. Sulfur phase and sulfur removal in high sulfur-containing bauxite. *Trans. Nonferr. Met. Soc.* **2011**, *21*, 1641–1647. [[CrossRef](#)]
3. Liu, Z.; Li, W.; Ma, W.; Yin, Z.; Wu, G. Conversion of sulfur by wet oxidation in the bayer process. *Metall. Mater. Trans. B* **2015**, *46*, 1702–1708. [[CrossRef](#)]
4. Yin, J.; Xia, W.; Han, M. Resource utilization of high-sulfur bauxite of low-median grade in Chongqing China. *Light Metal* **2011**, *49*, 19–22.
5. Chen, W.M.; Xie, Q.L.; Hu, X.L. Experimental study on reverse flotation technique for desulfurizing of high-sulfur bauxite. *Min. Metall. Eng.* **2008**, *28*, 34–37.
6. Padilla, R.; Vega, D.; Ruiz, M.C. Pressure leaching of sulfidized chalcopyrite in sulfuric acid-oxygen media. *Hydrometallurgy* **2007**, *86*, 80–88. [[CrossRef](#)]
7. Long, X.; Chen, J.; Chen, Y. Adsorption of ethyl xanthate on ZnS(110) surface in the presence of water molecules: A DFT study. *Appl. Surf. Sci.* **2016**, *370*, 11–18. [[CrossRef](#)]
8. Padmanabhan, N.P.H.; Sreenivas, T.; Rao, N.K. Processing of ores of titanium, zirconium, hafnium, niobium, tantalum, molybdenum, rhenium, and tungsten: International trends and the Indian scene. *High Temp. Mat. Process.* **1990**, *9*, 217–248. [[CrossRef](#)]

9. Wang, X.H.; Forssberg, K.S.E. Mechanisms of pyrite flotation with xanthates. *Int. J. Miner. Process.* **1991**, *33*, 275–290. [[CrossRef](#)]
10. Buckley, A. A survey of the application of X-ray photoelectron spectroscopy to flotation research. *Colloid Surf. A* **1994**, *93*, 159–172. [[CrossRef](#)]
11. Nagaraj, D.R.; Brinen, J.S. Sims study of adsorption of collectors on pyrite. *Int. J. Miner. Process.* **2001**, *63*, 45–57. [[CrossRef](#)]
12. Cao, F.; Sun, C.Y.; Wang, H.J.; Chen, F.W. Effect of alkyl structure on the flotation performance of xanthate collectors. *J. Univ. Sci. Technol. B* **2014**, *36*, 1589–1594.
13. Wang, X.M.; Zhang, T.A.; Lv, G.Z.; Dou, Z.H.; Li, B.; Jiang, X.L. Application comparison of xanthate flotation collectors in high-sulfur bauxite flotation desulfurization. *Chin. J. Process. Eng.* **2010**, *10*, 7–12.
14. Chen, S.H.; Gong, W.Q.; Mei, G.J.; Chen, X.D.; Yan, H.Z. Evaluation of biodegradability of alkyl xanthates flotation collectors. *J. Cent. South Univ.* **2011**, *42*, 546–554.
15. Xu, Y.; Liu, Y.L.; Gao, S.; Jiang, Z.W.; Su, D.; Liu, G.S. Monolayer adsorption of dodecylamine surfactants at the mica/water interface. *Chem. Eng. Sci.* **2014**, *114*, 58–69. [[CrossRef](#)]
16. Yazdanyar, A.; Aschauer, U.; Bowen, P. Interaction of biologically relevant ions and organic molecules with titanium oxide (rutile) surfaces: A review on molecular dynamics studies. *Colloid Surf. B* **2017**, *161*, 563–577. [[CrossRef](#)] [[PubMed](#)]
17. Tian, S.; Erastova, V.; Lu, S.; Greenwell, H.C.; Underwood, T.; Xue, H.; Zeng, F.; Chen, G.; Wu, C.; Zhao, R. Understanding model crude oil component interactions on kaolinite silicate and aluminol surfaces: Towards improved understanding of shale oil recovery. *Energy Fuels* **2017**, *32*, 1155–1165. [[CrossRef](#)]
18. Nikjoo, H.; O'Neill, P.; Wilson, W.E.; Goodhead, D.T. Computational approach for determining the spectrum of DNA damage induced by ionizing radiation. *Radiat. Res.* **2001**, *156*, 577–583. [[CrossRef](#)]
19. Wang, L.; Hu, Y.; Sun, W.; Sun, Y. Molecular dynamics simulation study of the interaction of mixed cationic/anionic surfactants with muscovite. *Appl. Surf. Sci.* **2015**, *327*, 364–370. [[CrossRef](#)]
20. Montalti, M.; Fornasiero, D.; Ralston, J. Ultraviolet-visible spectroscopic study of the kinetics of adsorption of ethyl xanthate on pyrite. *J. Colloid Interface Sci.* **1991**, *143*, 440–450. [[CrossRef](#)]
21. Tariq, M.; Freire, M.G.; Saramago, B.; Coutinho, J.A.; Lopes, J.N.; Rebelo, L.P. Surface tension of ionic liquids and ionic liquid solutions. *Chem. Soc. Rev.* **2012**, *41*, 829–868. [[CrossRef](#)] [[PubMed](#)]
22. And, G.L.; Watson, P.R. Surface tension measurements of N-alkylimidazolium ionic liquids. *Langmuir* **2001**, *17*, 6138–6141.
23. Xu, L.; Hu, Y.; Tian, J.; Wu, H.; Wang, L.; Yang, Y.; Wang, Z. Synergistic effect of mixed cationic/anionic collectors on flotation and adsorption of muscovite. *Colloid Surf. A* **2016**, *492*, 181–189. [[CrossRef](#)]
24. Dong, B.; Li, N.; Zheng, L.; Yu, L.; Inoue, T. Surface adsorption and micelle formation of surface active ionic liquids in aqueous solution. *Langmuir* **2007**, *23*, 4178–4182. [[CrossRef](#)] [[PubMed](#)]
25. Rappe, A.K.; Casewit, C.J.; Colwell, K.S.; Iii, W.A.G.; Skiff, W.M. Uff, a full periodic table force field for molecular mechanics and molecular dynamics simulations. *J. Am. Chem. Soc.* **1992**, *114*, 10024–10035. [[CrossRef](#)]
26. Zhao, C.; Chen, J.; Long, X.; Guo, J. Study of H₂O adsorption on sulfides surfaces and thermokinetic analysis. *J. Ind. Eng. Chem.* **2014**, *20*, 605–609. [[CrossRef](#)]
27. Underwood, T.; Erastova, V.; Greenwell, H.C. Wetting effects and molecular adsorption at hydrated kaolinite clay mineral surfaces. *J. Phys. Chem. C* **2016**, *120*, 11433–11449. [[CrossRef](#)]
28. Nosé, S. A unified formulation of the constant temperature molecular dynamics methods. *J. Chem. Phys.* **1984**, *81*, 511–519. [[CrossRef](#)]
29. Karasawa, N.; Iii, W.A.G. Acceleration of convergence for lattice sums. *J. Chem. Phys.* **1989**, *93*, 7320–7327. [[CrossRef](#)]
30. Williams, D.E. Accelerated convergence of crystal-lattice potential sums. *Acta Crystallogr. E* **1971**, *27*, 452–455. [[CrossRef](#)]
31. Pradip; Rai, B.; Rao, T.K.; Krishnamurthy, S.; Vetrivel, R.; Mielczarski, J.; Cases, J.M. Molecular modeling of interactions of diphosphonic acid based surfactants with calcium minerals. *Langmuir* **2002**, *18*, 932–940. [[CrossRef](#)]
32. Xu, L.; Hu, Y.; Dong, F.; Gao, Z.; Wu, H.; Wang, Z. Anisotropic adsorption of oleate on diasporite and kaolinite crystals: Implications for their flotation separation. *Appl. Surf. Sci.* **2014**, *321*, 331–338. [[CrossRef](#)]

33. Qiang, Y.; Zhang, S.; Xu, S.; Yin, L. The effect of 5-nitroindazole as an inhibitor for the corrosion of copper in a 3.0% NaCl solution. *Rsc Adv.* **2015**, *5*, 63866–63873. [[CrossRef](#)]
34. Ulman, A. Formation and structure of self-assembled monolayers. *Chem. Rev.* **1996**, *96*, 1533. [[CrossRef](#)] [[PubMed](#)]
35. Somasundaran, P.; Wang, D. Chapter 5 application of flotation agents and their structure-property relationships. *Dev. Miner. Process.* **2006**, *17*, 143–201.
36. Liu, G.; Yang, X.; Zhong, H. Molecular design of flotation collectors: A recent progress. *Adv. Colloid Interface Sci.* **2017**, *246*, 181–195. [[CrossRef](#)] [[PubMed](#)]
37. Rueda, J.A.; Ruffini, R.; Wu, Y.B.; Xue, S.S. Surface tension of the core-crust interface of neutron stars with global charge neutrality. *Phys. Rev. C* **2014**, *89*, 196–204. [[CrossRef](#)]
38. Monte, M.B.M.; Lins, F.F.; Oliveira, J.F. Selective flotation of gold from pyrite under oxidizing conditions. *Int. J. Miner. Process.* **1997**, *51*, 255–267. [[CrossRef](#)]
39. Aristilde, L.; Sposito, G. Molecular modeling of metal complexation by a fluoroquinolone antibiotic. *Environ. Toxicol. Chem.* **2008**, *27*, 2304–2310. [[CrossRef](#)] [[PubMed](#)]
40. Rosso, K.M.; Becker, U.; Hochella, M.F. Atomically resolved electronic structure of pyrite {100} surfaces; an experimental and theoretical investigation with implications for reactivity. *Am. Mineral.* **1999**, *84*, 1535–1548. [[CrossRef](#)]
41. Dewar, M.J.S. A critique of frontier orbital theory. *J. Mol. Struct. Theochem.* **1989**, *200*, 301–323. [[CrossRef](#)]
42. Li, Y.Q.; Chen, J.H.; Chen, Y.; Guo, J. Density functional theory study of influence of impurity on electronic properties and reactivity of pyrite. *Trans. Nonferr. Met. Soc. China* **2011**, *21*, 1887–1895. [[CrossRef](#)]
43. Guo, L.; Zhu, S.; Zhang, S.; He, Q.; Li, W. Theoretical studies of three triazole derivatives as corrosion inhibitors for mild steel in acidic medium. *Corros. Sci.* **2014**, *87*, 366–375. [[CrossRef](#)]
44. Khaled, K.F.; Hamed, M.N.H.; Abdel-Azim, K.M.; Abdelshafi, N.S. Inhibition of copper corrosion in 3.5% nacl solutions by a new pyrimidine derivative: Electrochemical and computer simulation techniques. *J. Solid State Electrochem.* **2011**, *15*, 663–673. [[CrossRef](#)]



© 2018 by the authors. Licensee MDPI, Basel, Switzerland. This article is an open access article distributed under the terms and conditions of the Creative Commons Attribution (CC BY) license (<http://creativecommons.org/licenses/by/4.0/>).